ANL/MSD/CP--77907

DE93 004154

Computer Simulation of the Anomalous Elastic Behavior of Thin Films and Superlattices*

D. Wolf
Material Science Division
Argonne National Laboratory
Argonne, IL 60439

October 1992

*This work was supported by the U.S. Department of Energy, BES Materials Sciences, under Contract W-31-109-Eng-38.

Manuscript to be published in the Proceedings of the Second International Conference on Computer Applications to Materials and Molecular Science and Engineering (CAMSE '92), Tokyo, Japan, Sept. 22-25, 1992.

DISCLAIMER

Computer Simulation of the Anomalous Elastic Behavior of Thin Films and Superlattices

D. Wolf

Materials Science Division, Argonne National Laboratory
Argonne, IL 60439.

Atomistic simulations are reviewed that elucidate the causes of the anomalous elastic behavior of thin films and superlattices (the so-called supermodulus effect). The investigation of free-standing thin films and of superlattices of grain boundaries shows that the supermodulus effect is not an electronic but a structural interface effect intricately connected with the local atomic disorder at the interfaces. The consequent predictions that (i) *coherent* strained-layer superlattices should show the smallest elastic anomalies and (ii) the introduction of incoherency at the interfaces should enhance all anomalies are validated by simulations of dissimilar-material superlattices.

1. INTRODUCTION

The discovery [1] and intensive investigation in recent years [2,3] of anomalies in the elastic response of multilayer metal films has given rise to hopes that one day it may be possible to develop synthetic layered materials with elastic properties not otherwise achievable. Whereas in many cases an elastic softening has been reported [3], in some instances a hardening has been observed [1, 4], although recent experiments (see, for example, [5-7]) have questioned the magnitudes of these strengthenings.

In superlattice materials in which detailed x-ray studies exist, the elastic anomalies were found to be accompanied by structural changes. [2,3,5-8] In general, an expansion in the z direction (parallel to the interface-plane normal) is observed which, in cases in which experiments were performed, is accompanied by anisotropic lattice-parameter changes in the interface (x-y) plane. Whereas the expansion in the z direction can obviously explain [8] both the observed softening of the shear elastic constant C_{44} (for shear parallel to the interface plane) [3] and a sometimes observed softening of C_{33} (parallel to z) [5], the *strengthening* reported in Young's and the biaxial modulus [1, 4] appears to be in conflict with these elastic-constant measurements particularly since it is well known that in bulk crystals a lattice expansion is usually accompanied by a *softened* elastic response. Again we mention, however, that a consensus as to the magnitudes of these strengthenings has not emerged from the experiments.

Two qualitative explanations based on electronic structure arguments [9,10] have been offered to account for the observed existence of elastic and structural anomalies in strained-layer superlattices. In one a finite-size effect giving rise to a folding back of the Brillouin zone is assumed to be responsible [9]; in the other the different electronic properties of the constituents are assumed to produce strains in the z direction distributed homogeneously throughout the bulk of the multilayer film [10]. Both models thus assume the anomalies to be a homogeneous electronic effect. However, recent experimental evidence [5,11-13] strongly suggests that the expansion in the z direction is localized at the interfaces.

Other explanations put forward invoke arguments based on continuum elasticity [14] or the third-order elastic constants of anisotropically strained systems [15]. Similar to the electronic-structure arguments, by treating the superlattice as a homogeneous system, the latter also ignore the role of the interfaces as structural defects. Although these and other efforts [8,16] have reproduced various aspects of the structure and elastic behavior of superlattices, given the structural and chemical complexity of these materials it is not surprising that these studies have revealed little about the underlying physical causes.

Here we focus on the structural causes for the anomalous elastic behavior of multilayers. The detailed investigation of thin films and of superlattices of grain boundaries (see Sec. 3) shows that the supermodulus effect is not an electronic nor a homogeneous effect but, instead, a structural interface effect

intricately connected with the local (i.e., inhomogeneous) atomic disorder at the interfaces. The consequent predictions that (i) *coherent* strained-layer superlattices should exhibit the smallest elastic anomalies and (ii) making the interfaces incoherent should enhance all anomalies are validated by simulations of dissimilar-material superlattices (see Sec. 4). The effect of temperature will be discussed in Sec. 5.

2. COMPUTATIONAL METHODS

Since virtually all elastic-property measurements on strained-layer superlattices have been performed at rather low temperatures, two atomistic simulation codes appropriate for T = 0 studies are used in our computer calculations in Secs. 3 and 4. For a given value of the modulation wavelength, Λ, the structure is first relaxed under zero external stress, followed by a lattice-dynamics like evaluation of the elastic-constant tensor. The constant-pressure relaxation procedure permits the unit-cell volume to respond to the internal pressure, thus allowing the superlattices to expand in the z direction and to contract or expand in the x-y plane. [17] Following the complete relaxation of the system, the 6 x 6 elastic-constant and -compliance tensors at T=0 are evaluated using a lattice-dynamics like method. [18] The elastic constants thus obtained can be compared directly with those extracted from stress-strain curves.

A non-trivial conceptual problem in the evaluation of elastic constants for *inhomogeneous* systems arises from the internal relaxations which occur following the application of an external strain or stress to the system. This relaxation effect, absent when homogeneously deforming, for example, a perfect monatomic cubic crystal, gives rise to a contribution to the zero-temperature elastic constants, in addition to the well-known Born term [19]. In molecular dynamics simulations of elastic constants (see also Sec. 5) this relaxation contribution is part of the so-called fluctuation term [20] which, for inhomogeneous systems, does not vanish in the T→0 limit.

In all simulations discussed below a Lennard-Jones (LJ) pair potential fitted for Cu and an embedded-atom-method (EAM) potential fitted for Au [21] will be used. As discussed in detail elsewhere [22], the two types of potentials yield qualitatively the same behavior for most interfacially controlled materials properties, indicating that the properties of interfaces are dominated by the (central-force) repulsive interactions in these potentials. Here we will therefore use the two types more or less interchangably.

3. STRUCTURE AND ELASTIC BEHAVIOR OF THIN FILMS AND SUPERLATTICES OF GRAIN BOUNDARIES

As already mentioned, the simultaneous presence of structural and chemical disorder at the interfaces in real materials greatly complicates the interpretation of any lattice-parameter changes or elastic anomalies observed either experimentally or in computer simulations. By first investigating the structure and elastic behavior of free-standing thin films and superlattices of grain boundaries (admittedly two extremely simple model systems), we eliminate chemistry as a factor. This simplification permits us to focus on the correlation between the atomic structure at the interfaces on one hand and the elastic behavior on the other.

3.1. Thin Films

It has been widely recognized in recent years that the surface-stress tensor, $\sigma_{\alpha\beta}$ (α,β=x,y,z), may play an important role in the structure and elastic response of thin films and superlattices. [17, 23-27] In a fully relaxed surface $\sigma_{\alpha\beta}$ is usually diagonal, with a vanishing component, σ_{zz}, in the direction of the surface normal (z direction). In many cases its only non-zero elements, σ_{xx} and σ_{yy}, are tensile (indicated by negative values) [23, 28], and of significant magnitude, favoring contraction in the (x-y) plane of the surface.

While in a bulk free surface this stress can only be relaxed, for example, by reconstruction or segregation [23], a thin film may in addition contract, giving rise to a uniform reduction in the average lattice parameter(s) in the film plane (see Fig. 1), with a consequent Poisson expansion in the z direction.

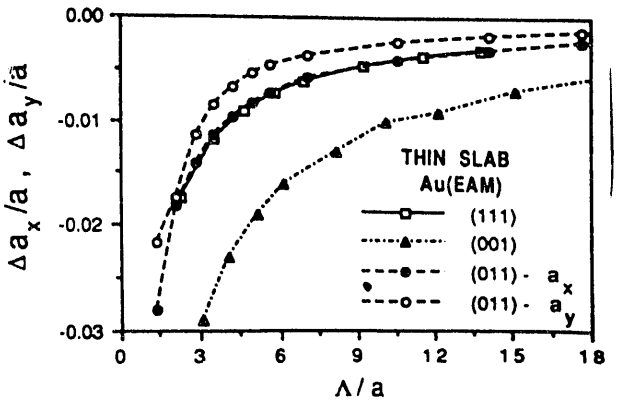

Figure 1. Surface-stress-induced in-plane contractions, $\Delta a_x/a$ and $\Delta a_y/a$ (<0), of unsupported thin films of Au. a is the cubic lattice parameter. [27]

To relate these strains quantitatively to the surface-stress tensor, in zero-th order the film stresses, $\sigma_{\alpha\beta}(\Lambda)$ and elastic constants, $C_{\alpha\beta}(\Lambda)$, (and hence the compliances, $S_{\alpha\beta}(\Lambda)=[C_{\alpha\beta}(\Lambda)]^{-1}$), may be approximated by their bulk values $\sigma^{\infty}_{\alpha\beta}$, $C^{\infty}_{\alpha\beta}$ and $S^{\infty}_{\alpha\beta}$ obtained in the $\Lambda\rightarrow\infty$ limit; here Λ represents the film thickness. Using linear elasticity theory, for the isotropic (001) and (111) films the in-plane contractions may be written as follows [27]:

$$\Delta a_x/a = \Delta a_y/a \approx (1/\Lambda)\, \sigma^{\infty}_{xx} / Y^{\infty}_{b} \ , \qquad (1)$$

where $Y^{\infty}_{b}=[\, S^{\infty}_{11} + S^{\infty}_{12}\,]^{-1}$ is the biaxial modulus. Eq. (1) expresses the fact that a tensile surface stress ($\sigma^{\infty}_{xx}<0$) gives rise to an in-plane contraction ($\Delta a_x, \Delta a_y < 0$).

As a consequence of the Poisson effect, the in-plane contraction has a pronounced effect on the film structure in the z direction. Considering that σ_{zz} vanishes identically for any value of Λ, analogous to Eq. (1) the Poisson strain, $\Delta a_z/a$, is given by

$$\Delta a_z/a \approx [\, \sigma^{\infty}_{xx}\, S^{\infty}_{13} + \sigma^{\infty}_{yy}\, S^{\infty}_{23}\,] / \Lambda \ . \qquad (2)$$

Defining the Poisson ratios $\nu_{xy} = -S_{12}/S_{11}$ and $\nu_{zx} = -S_{13}/S_{11}$, for the isotropic (111) and (001) planes, with $S_{13} = S_{23}$, Eqs. (1) and (2) may be combined to yield:

$$\Delta a_z/a = -\, 2\, (\Delta a_x/a)\, \nu^{\infty}_{zx} / (1 - \nu^{\infty}_{xy}) \ . \qquad (3)$$

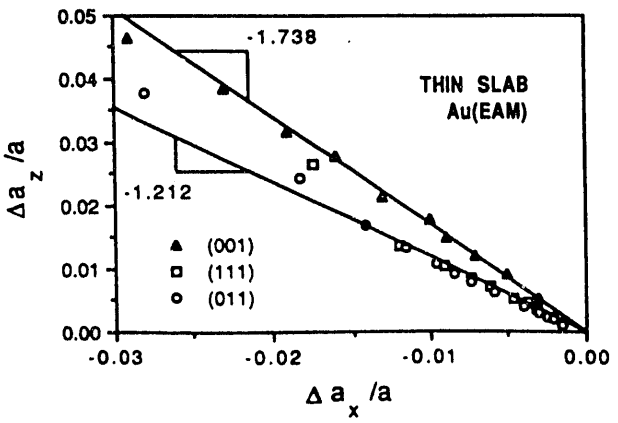

Figure 2. Poisson expansion, $\Delta a_z/a$ (>0), of the films in Fig. 1 (see also Eq. (3) below). [27]

As expected for the Poisson effect, the signs of Δa_z and Δa_x are opposite; for $\Delta a_x<0$ an *outward* displacement of the film surfaces is therefore expected ($\Delta a_z>0$).

To test the validity of Eq. (3), in Fig. 2 the values of $\Delta a_z/a$ determined in the manner described above are plotted against $\Delta a_x/a$. The solid lines in the figure, with slopes $-2\nu^{\infty}_{zx}/(1-\nu^{\infty}_{xy}) = -1.121$ and -1.738, respectively, are the predictions of Eq. (3) based on the bulk stresses and moduli. Their excellent representation of the simulation data demonstrates that, with the exception of the largest contractions (i.e., the smallest values of Λ, typically $\Lambda\leq 4a$), the zero-th order linear-elastic equations (1) - (3) permit prediction of the anisotropic lattice-parameter changes of a free-standing thin film based entirely on the knowledge of the *bulk*-surface stresses and the *perfect-crystal* moduli. (For further details see Ref. [27].)

It has been suggested that the decrease in the average atomic volume associated with these anisotropic lattice-parameter changes give rise to a strengthening of at least some elastic moduli, as one would expect for a homogeneous solid. [25] However, as evidenced by the related Young's moduli Y_x, Y_y, and Y_z shown in Figs. 3(a) and (b), while some moduli are, indeed, strengthened others are weakened. For example, in spite of the largest in-plane contraction observed for the (001) film (see Fig. 1), the related modulus Y_x ($=Y_y$) is weakened significantly (see Fig. 3(a)) while, surprisingly, Y_z simultaneously *strengthens*. By contrast, the behavior of the (111) film is more like that of a homogeneous material: the in-plane contraction is accompanied by a strengthening in Y_x, while the z expansion gives rise to a softening in Y_z. Interestingly, in the (011) film Y_x is practically independent of Λ while both Y_y and Y_z soften substantially.

In exploring the origin of this anomalous elastic behavior, it is important to recognize that, even without the stress-induced contractions in the film plane, the presence of the structurally disordered film surfaces alone alters the average elastic response of the film as a function of Λ; this response is then modified by the superimposed stress-induced lattice-parameter changes. Two contributions to the net elastic behavior therefore have to be distinguished. These can be separated by first determining the elastic constants of the thin film in which the x-y contraction

has been suppressed, against which the additional effects due to the in-plane contractions can then be probed. All three Young's moduli are then found to decrease steadily. [27] If now the surface stresses are also permitted to relax, the distinct effect of the in-plane contractions alone is given simply by the differences ΔY_x, ΔY_y and ΔY_z between these moduli and those in Fig. 3. [27]

A detailed analysis of these results [27] demonstrates that no direct relation exists between the surface-stress-induced anisotropic lattice-parameter changes and either the overall elastic moduli or the contribution due to the surface stress alone. The reasons for this very complex elastic behavior appear to be intricately connected with the rather complex nature of the coupling between the in-plane contractions and the consequent yielding of the material in the z direction. This coupling leads to a continuous modification of the detailed atomic structure of the film surfaces as Λ decreases, i.e., to a continuous

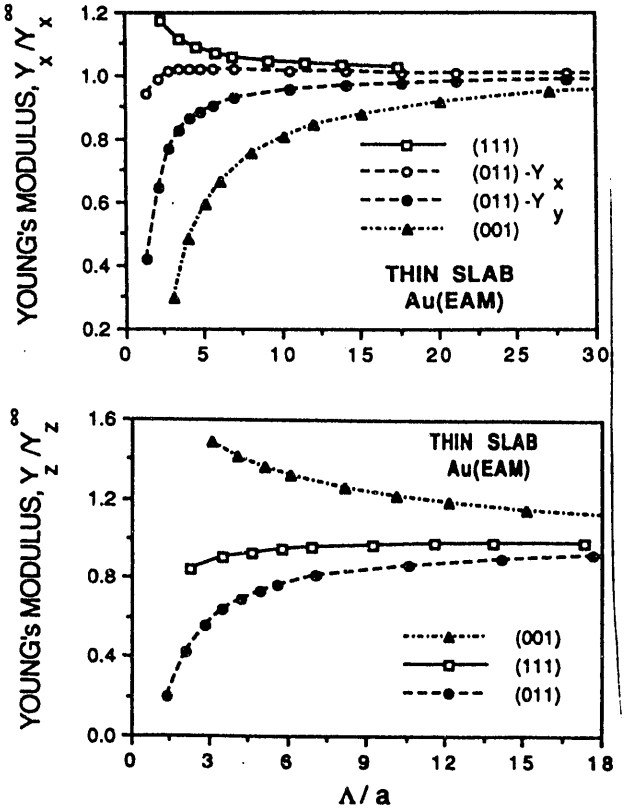

Figure 3. Young's moduli, Y_x,Y_y and Y_z of fully relaxed single-crystal films of Au, normalized to the related bulk values. [27]

evolution of the nature of the inhomogeneities near the film surfaces.

3.2. Grain-Boundary Superlattices (GBSLs)

As for the free-standing thin films discussed above, our detailed investigation of superlattices of grain boundaries (GBs) [17, 29-31] has demonstrated that the anisotropic changes in the *average* lattice parameters can be predicted approximately based on a knowledge of the interfacial-stress tensor and of bulk elastic constants [30]. Therefore, in this section we elaborate only on the relationship between the elastic anomalies and the underlying *atomic* structure (as seen, for example, in the radial distribution function). We will demonstrate that, as for the free-standing thin films, the observed elastic anomalies are a structural interface effect, and hence associated with the fact that superlattices are inhomogeneous systems.

If, as suggested in Sec. 3.1, the structural disorder localized at the interfaces is, indeed, the main cause for the anomalous elastic behavior of the system, one would expect a strong dependence of the magnitude of these anomalies on the interface energy. Our comparison between GBSLs composed of (100) and (111) twist boundaries is motivated by the fact that, based on their substantially lower energies [31], one would expect significantly smaller elastic anomalies for the (111) than for the (100) GBSLs.

Because a buried grain boundary is sandwiched between bulk material, the interfacial stress parallel to the GB (similar in nature to the surface stress) cannot be relaxed; i.e., a lateral contraction cannot occur. In a superlattice of GBs, by contrast, the size

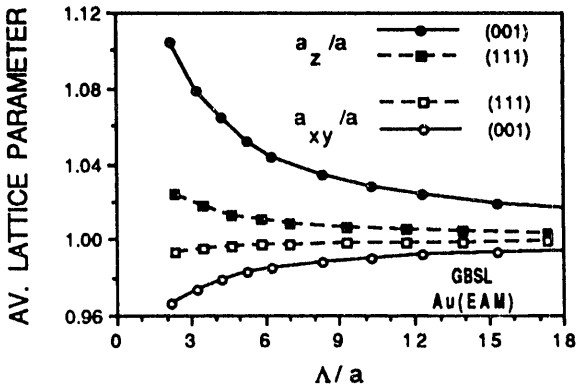

Figure 4. Average lattice parameters, a_{xy}/a and a_z/a, parallel and perpendicular to the interface planes vs. modulation wavelength, Λ (in units of the lattice parameter a). [29]

of the perfect-crystal regions surrounding the GBs is gradually reduced as Λ decreases, and the lateral contraction can actually take place. As illustrated in Fig. 4, the average x-y lattice parameter, $a_x=a_y=a_{xy}$, consequently decreases with decreasing Λ for both sets of GBSLs; by contrast, a_z increases because of the volume expansion at the GB [32] and because an ever larger volume fraction of atoms experiences the GBs as Λ becomes smaller.

Although generally rather small, the x-y contraction is substantially larger for the superlattices on the (100) plane than for those on the (111) plane, for which almost no contraction in the interface plane is observed. This difference arises from the very different energies - and hence volume expansions [32] - of the related GBs: the larger volume expansion for the (100) boundaries [32] gives rise to a much larger interface stress which, when relaxed, results in a much larger Poisson contraction.

The elastic moduli exhibiting the largest anomalies that were obtained for the two sets of GB superlattices, with full consideration of the relaxation-term elastic-constant contribution [18], are summarized in Figs. 5 and 6. (Other moduli can also be determined readily, as discussed in detail in Ref. [17] for the case of the (100) GBSLs.) The elastic constants and moduli in the $\Lambda\rightarrow\infty$ limit are governed by the averages over two perfect fcc crystals rotated with respect to one another about <100> or <111>, respectively [3]; they can be determined independently from the perfect-crystal elastic-constant tensor. Notice that the moduli in Figs. 5 and 6 have been normalized to these $\Lambda\rightarrow\infty$ values.

According to Figs. 5 and 6, Y_z increases with decreasing modulation wavelength while G_{xz} decreases dramatically. Particularly interesting is the long range over which $G_{xz}(\Lambda)$ is substantially reduced in both cases, as well as its very small values at the minima which appear at $\Lambda \approx 4a \approx 15$Å. These low values of G_{xz} at the minima indicate an extremely small shear resistance right at the interfaces. This extremely slow convergence in the shear moduli for $\Lambda\rightarrow\infty$ was shown to arise from a greatly reduced shear resistance at high-angle grain boundaries [33, 34].

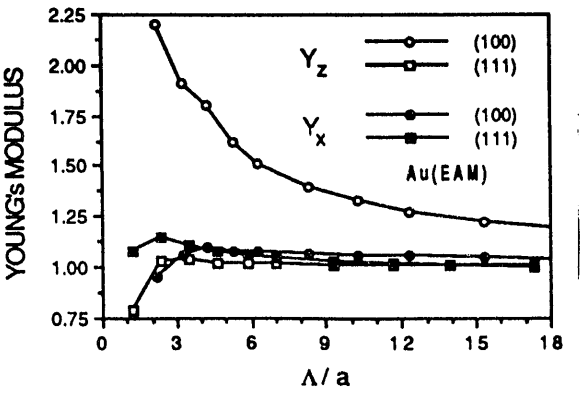

Figure 5. Normalized values of Young's moduli in the x and z directions for the (100) and (111) GBSLs.

The Young's moduli in Fig. 5 show a strong dependence on the GB plane. Most remarkably, in spite of the much larger z expansion of the (100) GBSLs by comparison with the (111) GBSLs (see Fig. 4), the related values of Y_z are significantly more strengthened. Equally puzzling, in spite of the much smaller x-y contraction of the (111) GBSLs (see Fig. 4), the related values of Y_x are significantly more strengthened than those for the (100) GBSLs. The shear moduli, by contrast, are of the same magnitude for the two different GB planes. Why, in contrast to Y_x and Y_z, the shear moduli are rather insensitive functions of the detailed atomic structure and energy of the GBs was discussed in detail in [29].

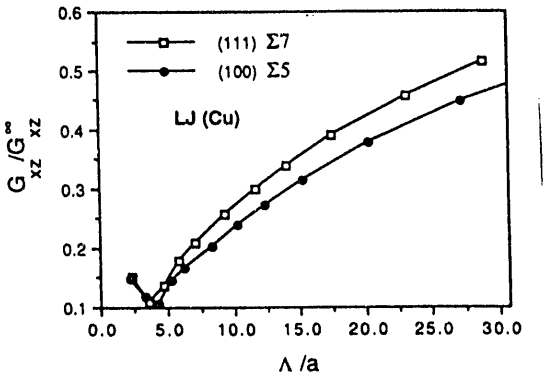

Figure 6. Normalized moduli for shear parallel to the interface planes for the (100) and (111) GBSLs. [29]

3.3. Discussion

Our simulations of free-standing thin films and superlattices of (100) and (111) twist grain boundaries demonstrate the existence of an intimate connection between the structural disorder at the interfaces (characterized, for example, by the GB energy) and the elastic anomalies of these systems. In particular, the replacement of the grain boundaries in a GBSL by the much less disordered free surfaces (i.e., the replacement of the superlattice by a single free-standing thin film) greatly reduces the elastic anomalies.

This reduction demonstrates an important point. Based on the observation that the thin films are actually *denser* than the perfect crystal, by contrast with the GBSLs (see Fig. 7), intuitively one would expect the slabs to be elastically *stronger* than the GBSLs. The above results demonstrate that this intuition, based on the behavior of a *homogeneous* system, is incorrect as are models based on homogeneous behavior [8,14,15,25]. It therefore appears that the supermodulus effect is a structural interface effect. In the following, we will further investigate the relationship between the atomic structure of the interfaces and the elastic anomalies.

The degree of structural disorder is best illustrated by radial distribution functions like the ones shown in Figs. 8(a) and (b) associated with the GBSLs on the (100) and (111) planes, each containing 6 lattice planes in the unit cell, i.e., three lattice planes each between the interfaces. The comparison of the substantially broadened peaks with the corresponding zero-temperature δ-function peaks of heights 12, 6, 24, etc. at the nearest-neighbor (nn), 2nd nn, 3rd nn, etc. distances of 0.707a, a, 1.225a, etc. demonstrates the strongly defected local environments of the atoms in the superlattices. A detailed analysis shows the peak centers to be shifted slightly towards larger distances [17, 31], by an amount approximately proportional to the corresponding volume expansion at the GBs. The greater broadening, combined with a larger shift, of the peaks associated with the (100) superlattices indicates the larger amount of disorder in these systems. A slice-by-slice analysis of these distribution functions (performed in Ref. [17] for the (100)

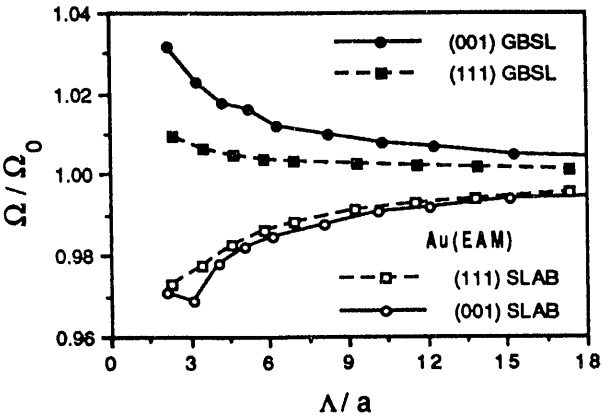

Figure 7. Average atomic volume vs. Λ for free-standing thin films and GBSLs. [27,28]

plane), and a detailed analysis of the interplanar separations in the superlattices [17] shows the disorder to be localized at the GBs.

The apparently paradoxical question, first addressed in Ref. [31], is this: How can at least some elastic moduli of an interface material *strengthen*, although the overall sample volume increases? Based on our usual intuition, gained from the study of *homogeneous* systems, one would expect all elastic moduli and constants to *weaken* upon expansion. As first pointed out in Ref. [31], although the overall volume of the system expands upon introduction of the interfaces (i.e., the *average* distance between the atoms *increases*), some atoms are in closer proximity to one-another, up to about 10%, than they are in the perfect crystal (see Fig. 8). These shorter distances are expected to *strengthen* the local elastic response whereas longer distances give rise to a *softening*, with the net effect being a strengthening of some moduli. However, as illustrated in Figs. 5 and 6, the

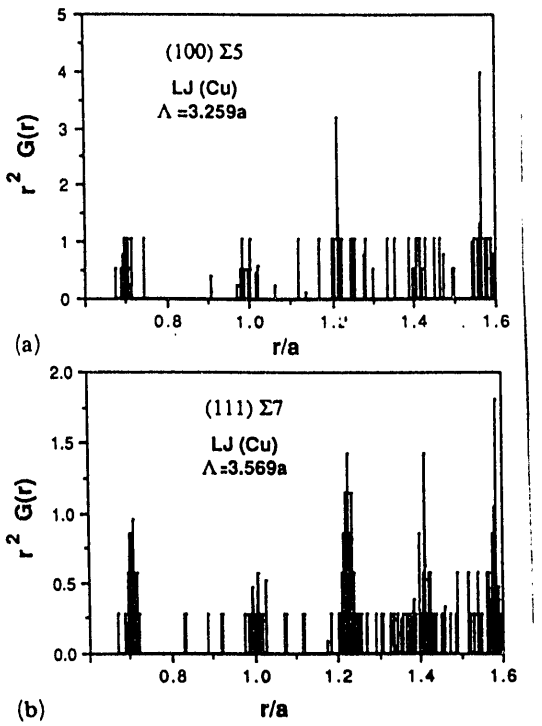

Figure 8. Radial distribution functions, $r^2G(r)$, associated with GB superlattices on the (100) (top) and (111) planes (bottom), respectively, each containing 6 lattice planes in the unit cell, i.e., three planes each between the interfaces. [29]

net outcome of this complex averaging process seems to depend strongly on the detailed atomic structure of the interfaces. The structural disorder at the interfaces therefore provides causes for both a strengthening and a softening of the elastic response, with the larger degree of disorder in the (100) superlattices causing the larger anomalies.

The above discussion exposes the very different roles played by the structural disorder and the consequent anisotropic lattice-parameter changes in the thin slabs and GBSLs: While the basic elastic anomalies of the system are caused by the structural disorder, the effect of the lattice-parameter changes is to enhance the anomalies due to the very existence of structural disorder. [17] In what follows, an attempt will be made to separate the two phenomena.

To illustrate the behavior of a *homogeneous* system, however under the effect of the anisotropic lattice-parameter changes discussed above, we have investigated the elastic properties of a perfect crystal subjected to the anisotropic lattice-parameter changes of the superlattices shown in Fig. 4, thus eliminating any effects due to the interfaces and the structural disorder associated with them. The results thus obtained, for example, for the moduli in Fig. 5 are shown in Fig. 9. (For a similar comparison for other moduli, see Ref. [29].)

In accordance with the volume increase in both types of superlattices (see Fig. 7), the Young's moduli of the homogeneously strained perfect crystal in Fig. 9 decrease monotonically as a function of Λ. The enhancements in Y_z (see Fig. 5) thus disappear completely with the elimination of the interfaces from the system. Similarly for the shear moduli [29],

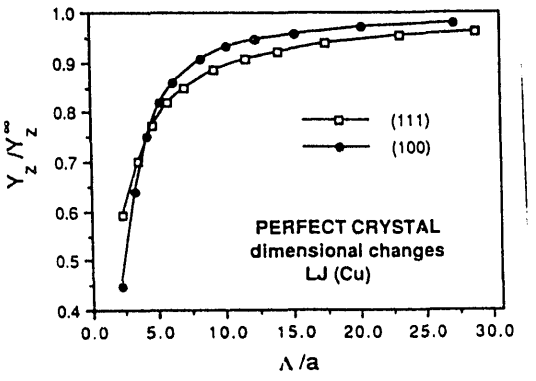

Figure 9. Normalized values of the Young's moduli in the z direction vs. Λ for perfect crystals of identical lattice parameters and planar orientations as the GBSLs in Fig. 4. [29]

no minima appear in the homoge-neously strained material, with much less dramatically softened shear moduli [29]. This comparison demonstrates that the enhancement of Y_z and the large softening in G_{xz} as well as the appearance of extremes in these moduli are intimately connected with the presence of interfaces in the system.

This comparison of the elastic behavior of homogeneous and inhomogeneous systems strongly suggests that models to explain the supermodulus effect based solely on the anisotropic lattice-parameter changes of strained-layer superlattice materials [8,15,25] may miss an important ingredient necessary for understanding supermodulus behavior, namely the important role played by the interfaces.

We finally consider the difference between the elastic constants and moduli, a rather fundamental distinction from both a conceptual and experimental viewpoint. When determining a *modulus*, an external *stress* is applied to the system and the ensuing strains are monitored; i.e., the stress is fixed and the strains are variables. In an elastic-*constant* measurement, by contrast, a *strain* is imposed on the system and the ensuing stresses are monitored. Hence, while a *modulus* describes the physical response of the system while permitting all lattice-parameter changes of the system in response to the applied stress to take place, an elastic *constant* describes the system response while all strains are fixed. The moduli are consequently given by the elastic compliances, thus representing combinations of elastic constants. Consequently, while the anomalies in the elastic constants may be rather small (see Fig. 9), the anomalies in the related moduli may be much larger by comparison. It therefore appears that the reduced elastic *constants* reported in numerous experiments may not be in total

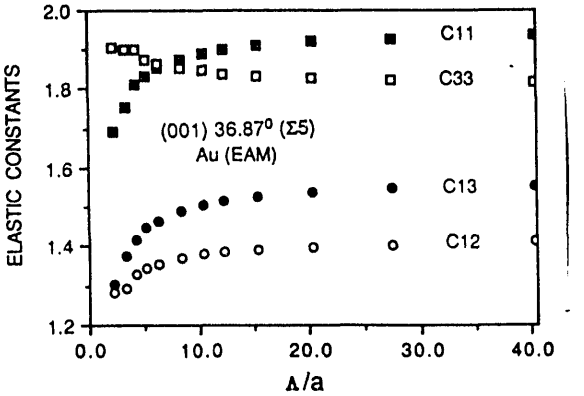

Figure 10. Elastic constants (in 10^{12} dyn/cm^2) for the (100) GBSLs(see also Fig. 5). [17,35]

contradiction to experiments in which enhanced *moduli* were observed. The super*modulus* effect may therefore be very aptly named since a "super *elastic-constant*" effect does not exist.

4. ROLE OF COHERENCY IN DISSIMILAR-MATERIAL SUPERLATTICES

As illustrated above, the replacement of the grain boundaries in a GBSL by the much less disordered free surfaces (i.e., the replacement of the superlattice by a single free-standing thin film) greatly reduces the elastic anomalies. Also, the reduction in the GB energy (by replacing (100) twist boundaries by boundaries on the (111) plane) leads to much smaller elastic anomalies. Based on the above interpretation of these phenomena as a structural interface effect, several predictions can be made. Most importantly, coherent (i.e., perfectly epitaxial) interfaces should exhibit the smallest elastic anomalies; re-introduction of structural disorder via misfit dislocations should increase these anomalies significantly, similar to the GBSLs studied above.

In order to test this prediction, we have investigated the role of coherency in the elastic behavior of composition-modulated superlattices of fcc metals. [35, 36] Again, in order to eliminate interface chemistry as much as possible as a contributing factor, these simulations were performed using Lennard-Jones potentials with a 10% [35] and 20% lattice-parameter mismatch [36] but with the same cohesive energies. The structures, energies, and elastic properties of coherent and incoherent (100) superlattices were computed as a function of the modulation wavelength and compared with those of coherent superlattices. As expected, the incoherent superlattices were found to be more structurally disordered and exhibited greater elastic anomalies than the coherent ones, a difference which cannot be accounted for by the overall anisotropic lattice-parameter changes of the superlattices alone [15, 25].

Our main conclusion is that increasing the structural disorder in the superlattices by increasing the lattice-parameter mismatch or by introducing a relative rotation between the two materials (thus introducing screw dislocations, as in the case of the GBSLs of twist boundaries) will dramatically enhance the small elastic anomalies present in the coherent system. (For details see Refs. [35, 36].)

That the transition from an incoherent to a coherent interface structure is, indeed, associated with a reduction in the elastic anomalies was recently verified experimentally. [12,13]

5. EFFECT OF TEMPERATURE

Finally, the effect of temperature in the supermodulus effect was investigated by molecular-dynamics simulation. [37] Most importantly, the effects of homogeneous (temperature-induced) and inhomogeneous (interface-induced) structural disorder on the thermoelastic properties of the (100) GBSLs (see Sec. 3.2) were compared as a function of the modulation wavelength. It was found that the elastic moduli of the GBSLs soften with increasing temperature as one would expect for *homogeneous* materials. Considering that the elastic anomalies arise from the *inhomogeneous* structural disorder localized at the interfaces, this result is somewhat a surprise.

In these simulations [37], by allowing thermal expansion in some cases and not in others, the explicit effects of the thermal expansion on the elastic properties were also explored. It was found that the thermal disordering on one hand and the consequent volume expansion on the other are in competition with one-another. In particular, it was shown that the basic causes for the anomalous elastic behavior of interface materials can be found even in a perfect crystal: Increasing the temperature (i.e., broadening the radial distribution function) without permitting the crystal to expand actually *strengthens* the elastic constants. In superlattices, by contrast, such a broadening in the radial distribution function is present even at zero temperature (see Fig. 8), leading to an elastic strengthening perpendicular to the interfaces provided the related volume expansion is not too large.

We conclude [37] that atomic-level structural disorder, be it homogeneous (i.e., temperature-induced) or inhomogeneous (e.g., interface-induced), can lead to elastic stiffening, provided that the related volume expansions do not dominate the elastic behavior and result in a softening. These simulations have lent further credence to the interpretation of the supermodulus effect as a structural phenomenon.

6. CONCLUSIONS

We have used the unique capabilities of atomic-level computer simulations to explore the physical origin of the so-called supermodulus effect in strained-layer superlattices. These simulations have provided valuable insights into (a) the atomic-level phenomena and processes governing interfacial elasticity and (b) the physical causes for the

supermodulus effect. Such atomic-level insights are difficult to obtain by experimental means or from theoretical methods based on continuum mechanics. The three major conclusions of this work may be summarized as follows.

First, by systematically investigating free-standing thin films and superlattices of grain boundaries, chemistry was eliminated as a factor that might otherwise contribute to the elastic behavior. The elastic anomalies observed for these model materials were found to be qualitatively similar to those observed experimentally for dissimilar-material superlattices, with some moduli hardened while others are softened. Moreover, our simulations have shown that the super*modulus* effect does not exist in the elastic *constants*; i.e., although the anomalies in the elastic constants may be very small, the related anomalies in the moduli (which represent combinations of the elastic constants) are generally much more pronounced. These results suggest strongly that

(a) the elastic anomalies arise from the atomic-level structural disorder localized at the interfaces and not from electronic causes; however, the latter might alter, and contribute in addition to, these anomalies; and

(b) a knowledge of the anisotropic changes in the average lattice parameter, although contributing to the elastic anomalies, is not sufficient to predict the elastic behavior even qualitatively.

Second, based on the interpretation that the elastic anomalies arise from the degree of the interfacial atomic-level structural disorder, several predictions have been made and verified by simulations. Most importantly, coherent (i.e., perfectly epitaxial) interfaces were shown to give rise to the smallest elastic anomalies; re-introduction of structural disorder via misfit dislocations increases these anomalies significantly. It was also predicted and verified that the replacement of the grain boundaries in a grain-boundary superlattice by much less disordered free surfaces (i.e., the replacement of the superlattice by a single free-standing thin film) greatly reduces the elastic anomalies. These simulations lend further credence to the interpretation of the supermodulus effect as a structural interface effect.

Third, the effect of temperature in the supermodulus effect has been investigated. It was found that the elastic moduli of grain-boundary superlattices soften with increasing temperature as one would expect for *homogeneous* materials. Considering that the elastic anomalies arise from the *inhomogeneous* structural disorder localized at the interfaces, this result is somewhat a surprise.

Ultimately the elastic anomalies of interface materials arise from a competition between structural disorder and the consequent (usually anisotropic) volume change. This competition can be seen even in a perfect crystal at finite temperature: Increasing the temperature (i.e., broadening the radial distribution function) without permitting the crystal to expand actually *strengthens* the elastic constants and moduli. In superlattices, by contrast, such a broadening in the radial distribution function is present even at zero temperature, leading to an elastic strengthening perpendicular to the interfaces provided the related volume expansion, and the associated elastic softening, is not too large.

Acknowledgments

This work was supported by the U.S. Department of Energy, BES Materials Sciences, under Contract W-31-109-Eng-38, and by the Office of Naval Research under Contract No. N00014-88-F-019.

REFERENCES

1. W. M. C. Yang, T. Tsakalakos, and J. E. Hilliard, J. Appl. Phys. **48** (1977) 876.
2. See, for example, I. K. Schuller, in *The Institute of Electrical and Electronics Engineers Ultrasonics Symposium*, 1985, edited by B. R. McAvoy, IEEE, New York, 1985, p. 1093, and references therein.
3. See, for example, M. Grimsditch, in *Topics in Applied Physics: Light Scattering in Solids V*, edited by M. Cardona and G. Guntherodt, Springer, Berlin, 1989, p. 285, and references therein.
4. U. Helmersson, S. Todorova, S. A. Barnett, and J.-E. Sundgren, J. Appl. Phys. **62** (1987) 491.
5. B. M. Clemens and G. L. Eesley, Phys. Rev. Lett. **61** (1988) 2356.
6. J. R. Dutcher, S. Lee, J. Kim, J. A. Bell, G. E. Stegeman and C. F. Falco, Mater. Sci. and Eng. B **6** (1990) 199.
7. B. M. Davis, D. N. Seidman, A. Moreau, J. B. Ketterson, J. Mattson and M. Grimsditch, Phys. Rev. B **43** (1991) 9304.
8. I. K. Schuller and A. Rahman, Phys. Rev. Lett. **50** (1983) 1377.
9. T. B. Wu, J. Appl. Phys. **53** (1982) 5265.
10. M. L. Hubermann and M. Grimsditch, Phys. Rev. Lett. **62** (1989) 1403.

11. W. R. Bennett, J. A. Leavitt, and C. M. Falco, Phys. Rev. B **35** (1987) 4199.
12. G. Carlotti, D. Fioretto, G. Socino, B. Rodmacq and V. Pelosin, J. Appl. Phys. **71** (1992) 4897.
13. E. E. Fullerton, I. K. Schuller, F. T. Parker, K. A. Svinarich, G. L. Eesley, R. Badra and M. Grimsditch, Phys. Rev. B (to be published).
14. A. Banerjea and J. R. Smith, Phys. Rev. B **35** (1987) 5413.
15. A. I. Jankowski and T. Tsakalakos, J. Phys. F **15** (1985) 1279; A. I. Jankowski, J. Phys. F **18** (1988) 413.
16. M. Imafuku, Y. Sasajima, R. Yamamoto and M. Doyama, J. Phys. F **16** (1986) 823.
17. D. Wolf and J. F. Lutsko, J. Mater. Res. **4** (1989) 1427.
18. J. F. Lutsko, J. Appl. Phys. **65** (1989) 2991.
19. M. Born and K. Huang, *Dynamical Theory of Crystal Lattices*, Clarendon Press, Oxford, 1954.
20. J. Ray and A. Rahman, J. Chem. Phys. **80** (1984) 4423, and Phys. Rev. B **32** (1985) 733.
21. S. M. Foiles, M. I. Baskes and M. S. Daw, Phys. Rev. B **33** (1986) 7983.
22. D. Wolf, J. F. Lutsko and M. Kluge, in *Atomistic Simulation in Materials - Beyond Pair Potentials*, edited by V. Vitek and D. J. Srolovitz, Plenum Press, New York, 1989, p. 245.
23. R. J. Needs, Phys. Rev. Lett. **58** (1987) 53.
24. D. Wolf in *Metal-Ceramic Interfaces*, edited by M. Ruhle, A. G. Evans, M. F. Ashby and J. P. Hirth, Pergamon Press, 1989, p. 52.
25. R. C. Cammarata and K. Sieradzki, Phys. Rev. Lett. **62** (1989) 2005.
26. D. Wolf, Surf. Sci. **225** (1990) 117.
27. D. Wolf, Appl. Phys. Lett. **58** (1991) 2081.
28. D. Wolf, Surf. Sci. **226** (1990) 389.
29. D. Wolf, Mater. Sci. and Eng. A **126** (1990) 1.
30. D. Wolf and J. A. Jaszczak, in *Materials Interfaces: Atomic-Level Structure and Properties*, edited by D. Wolf and S. Yip, Chapman and Hall, London, 1992, p. 364.
31. D. Wolf and J. F. Lutsko, Phys. Rev. Lett. **60** (1988) 1170.
32. D. Wolf, Acta Metall. **37** (1989) 1983.
33. M. D. Kluge, D. Wolf, J. F. Lutsko and S. R. Phillpot, J. Appl. Phys. **67** (1990) 2370.
34. D. Wolf and M. D. Kluge, Scripta Metall. Mater. 24 (1990) 907.
35. D. Wolf and J. F. Lutsko, J. Appl. Phys. **66** (1989) 1961.
36. J. A. Jaszczak, S. R. Phillpot and D. Wolf, J. Appl. Phys. **68** (1990) 4573.
37. J. A. Jaszczak and D. Wolf, J. Mater. Res. **6** (1991) 1207.
38. J. A. Jaszczak and D. Wolf, Phys. Rev. B **46** (1992) 2473.

END

DATE
FILMED
2/12/93